JACS
JOURNAL OF THE AMERICAN CHEMICAL SOCIETY
Article
pubs.acs.org/JACS

Electrochemical Investigations of the Mechanism of Assembly of the Active-Site H-Cluster of [FeFe]-Hydrogenases

Clare F. Megarity,[†] Julian Esselborn,[‡] Suzannah V. Hexter,[†] Florian Wittkamp,[§] Ulf-Peter Apfel,[§] Thomas Happe,[‡] and Fraser A. Armstrong*[,†]

[†]Inorganic Chemistry Laboratory, Department of Chemistry, University of Oxford, South Parks Road, Oxford OX1 3QR, United Kingdom

[‡]Lehrstuhl für Biochemie der Pflanzen, AG Photobiotechnologie and [§]Lehrstuhl für Anorganische Chemie I, Ruhr-Universität Bochum, 44801 Bochum, Germany

Supporting Information

ABSTRACT: Protein film electrochemistry (PFE) has been used to study the assembly of the complex 6Fe active site of [FeFe]-hydrogenases (known as the H-cluster) from its precursors—the [4Fe-4S] domain that is already coordinated within the host, and the 2Fe domain that is presented as a synthetic water-soluble complex stabilized by an additional CO. Not only does PFE allow control of redox states via the electrode potential but also the immobilized state of the enzyme facilitates control of extremely low concentrations of the 2Fe complex. Results for two enzymes, *Cr*HydA1 from *Chlamydomonas reinhardtii* and *Cp*I from *Clostridium pasteurianum*, are very similar, despite large differences in size and structure. Assembly begins with very tight binding of the 34-valence electron 2Fe complex to the apo-[4Fe-4S] enzyme, well before the rate-determining step. The precursor is trapped under highly reducing conditions (<−0.5 V vs SHE) that prevent fusion of the [4Fe-4S] and 2Fe domains (via cysteine-S) since the immediate product would be too electron-rich. Relaxing this condition allows conversion to the active H-cluster. The intramolecular steps are relevant to the final stage of biological H-cluster maturation.

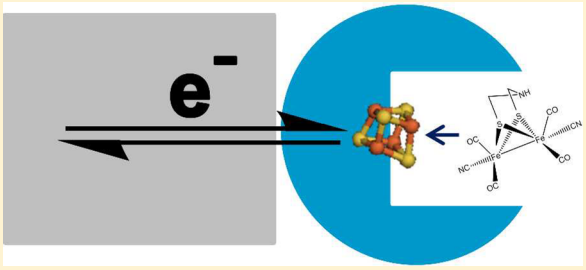

INTRODUCTION

The active site of [FeFe]-hydrogenases, known as the "H-cluster" (**I**, constructed from pdb 2C8Y), consists of two components—an unusual [2Fe] complex, containing diatomic ligands CO and CN^- and a bridging azadithiolate, which is the site of formation or oxidation of H_2, and a [4Fe-4S] cluster, coordinated by four cysteine thiolates, which can store one electron during catalysis.[1] The two subcomplexes are connected by one of the cysteine thiolates (μ-SCys) which also provides the only covalent link between the [2Fe] complex and the protein: the broken line shows the division between the two components.

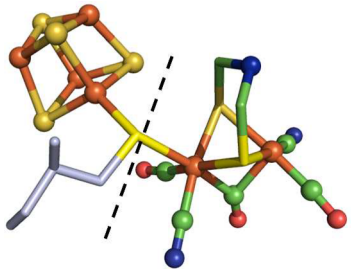

I

During biosynthesis the 2Fe complex is transferred to its awaiting recipient, the [4Fe-4S] "apoenzyme", from a scaffold protein, HydF, which houses the 2Fe complex as assembled from its simpler components through the action of two other maturation proteins HydE and HydG.[2,3] Two [FeFe]-hydrogenases have been under particular scrutiny regarding H-cluster assembly, namely, *Cr*HydA1 from the green algae *Chlamydomonas reinhardtii* and *Cp*I from the fermentative anaerobe *Clostridium pasteurianum*. Whereas *Cr*HydA1 contains only the H-cluster, *Cp*I is a more complex enzyme that also contains a relay system of four additional FeS clusters to mediate intramolecular electron transfer to and from the H-cluster. Crystallographic comparisons between *Cp*I and apo-[4Fe-4S] *Cp*I show that insertion of the 2Fe subcomplex does not greatly change the overall protein structure: in contrast, the only structure so far obtained for *Cr*HydA1 is of the apo-[4Fe-4S] form which has an open channel leading to the [4Fe-4S] cluster.[4,5] Hence it is possible, but uncertain at this stage, that both apo-[4Fe-4S] enzymes exist as open and closed states in equilibrium.

It was recently discovered[6] that a synthetic CO-adduct of the [2Fe] subcluster $[Fe_2[\mu\text{-}(SCH_2)_2NH](CN)_2(CO)_4]^{2-}$ (abbreviated $[2Fe]^{MIM}$, **II**) originally synthesized by Rauchfuss and co-workers[7] reacts *directly* with apo-[4Fe-4S] enzymes to yield active hydrogenases,[8] providing a new investigative route for H-cluster assembly.

Received: September 6, 2016
Published: October 24, 2016

DOI: 10.1021/jacs.6b09366
J. Am. Chem. Soc. 2016, 138, 15227−15233

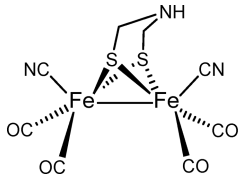

II

It is now recognized that [FeFe]-hydrogenases have exceptional electrocatalytic activity when attached to a suitable electrode.[9−15] Protein film electrochemistry (PFE) is a suite of techniques that allows detailed investigations of redox enzymes under conditions of controlled electrode potential, and the minuscule sample requirement ($\ll 10^{-12}$ mole for a typical electrode) makes it possible to control and observe equilibria at very high dilution.[16] We now report the application of PFE to investigate the final stages of H-cluster assembly in [FeFe]-hydrogenases, using $[2Fe]^{MIM}$ *in vitro* but with a view that the process entails steps close or equivalent to the events happening during final H-cluster maturation *in vivo*. To establish generalizations, we have studied H-cluster assembly in both *Cr*HydA1 and *Cp*I.

RESULTS AND DISCUSSION

Figure 1 shows a simple cyclic voltammetry experiment: a rotating disc pyrolytic graphite "edge" (PGE) electrode

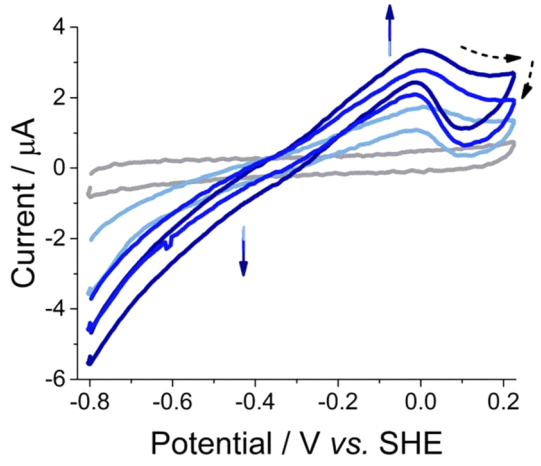

Figure 1. Cyclic voltammograms showing the activation of apo-*Cr*HydA1 adsorbed on a PGE electrode following injection of $[2Fe]^{MIM}$ (final concentration 0.2 μM) after cycle shown in gray. Conditions 5 °C, 100% H_2, 50 mM Na phosphate, 0.1 M NaCl pH 6.0. Scan rate: 30 mV s^{-1}. Broken arrows show direction of cycling.

modified by adsorption of a film of apo-*Cr*HydA1 (2 μL of 25 μM enzyme spotted onto the electrode surface then rinsed) was placed in the electrochemical cell solution, and an aliquot of $[2Fe]^{MIM}$ (final concentration 0.2 μM) was injected. Successive cycles reveal the formation of active hydrogenase, as evidenced by increasing H_2 oxidation and H^+ reduction currents on each side of the equilibrium potential. The inactivation and reactivation at high potential is due to well-documented formation of an oxidized inactive state.[10,13,17]

Figure 2 shows a comparison of the time dependence of the formation of active enzyme from precursors, measured either by a conventional solution assay or by chronoamperometry (CA) at a fixed electrode potential. In the conventional assay, benzyl viologen is reduced by H_2 (1 bar) at a rate proportional to the amount of active hydrogenase generated. Injection of

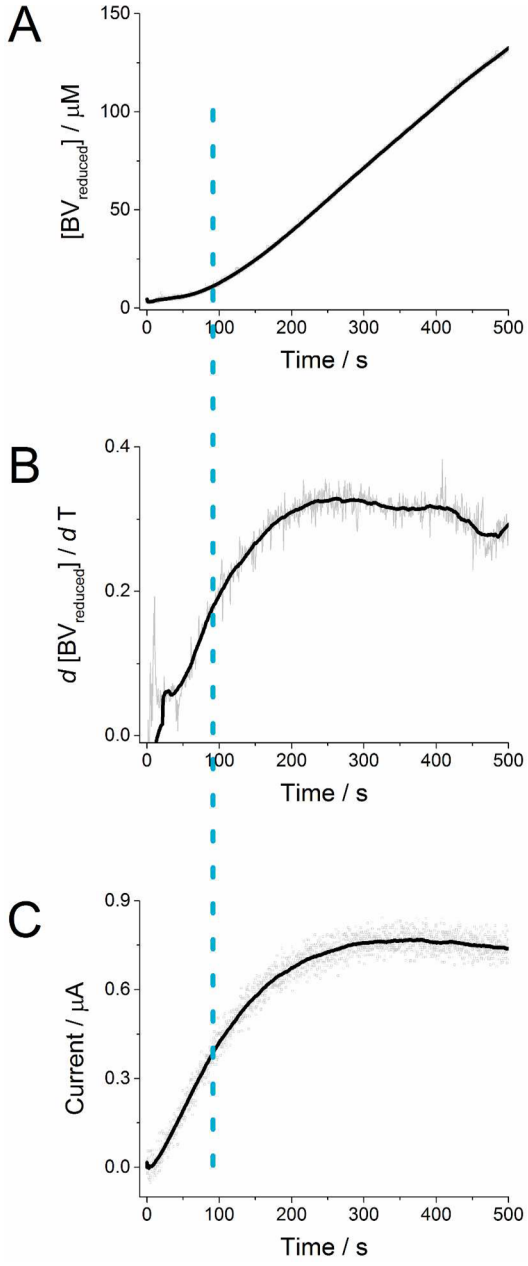

Figure 2. Recording H-cluster assembly in *Cr*HydA1 through the increase in H_2 oxidation activity at 1 bar H_2. (A) Solution experiment, monitoring benzyl viologen reduction at 600 nm: 10 nM apo-*Cr*HydA1; 0.1 μM $[2Fe]^{MIM}$ injected at t = 0; 20 °C; 0.1 M potassium phosphate pH 6.8. (B) First derivative of plot in (A). (C) CA experiment; $[2Fe]^{MIM}$ injected at t = 0 to final concentration of 50 nM; 0.1 M potassium phosphate pH 6.8; 20 °C, electrode potential = −0.04 V vs SHE. The vertical line marks the approximate half-life of the activation process.

$[2Fe]^{MIM}$ into the solution of 10 nM apo-[4Fe-4S] hydrogenase initiates the reduction of viologen that accelerates from zero to reach a steady rate (Figure 2A). This activation phase was analyzed by taking the derivative (Figure 2B), which yielded a half-life of approximately 1 min. Figure 2C shows a CA experiment carried out under equivalent conditions. Importantly, the current amplitude is directly proportional to enzyme activity, so the CA time course thus records the "rate of change of rate", i.e., as given by the derivative in the conventional assay. The rotating disc PGE electrode modified with a film of apo-

DOI: 10.1021/jacs.6b09366
J. Am. Chem. Soc. 2016, 138, 15227−15233

[4Fe-4S] enzyme was placed in 4 mL of solution; an electrode potential of −0.04 V vs SHE was applied; and $[2Fe]^{MIM}$ was injected to initiate the reaction. Rates of incorporation of $[2Fe]^{MIM}$ into apo-*Cr*HydA1, as measured by solution kinetics or CA, were compared using various concentrations of $[2Fe]^{MIM}$ (Table 1). The solution experiments were carried out at various enzyme concentrations, with $[2Fe]^{MIM}$ always in 10-fold excess. The CA experiments were repeated for different concentrations of $[2Fe]^{MIM}$. A typical coverage of enzyme on PGE is $<10^{-12}$ mol/cm^2; thus with electrode area 0.03 cm^2, the amount of enzyme in the CA experiments is <0.03 pmol. Therefore, $[2Fe]^{MIM}$ is always present at an amount well in excess of the apoenzyme.

Table 1. Rate Constants for Activation of *Cr*HydA1 Determined from the Lag Phase in Steady-State Solution Kinetics and from Chronoamperometry (Voltage Held at −0.04 V vs SHE for *Cr*HydA1 and −0.198 V vs SHE for *Cp*I) at 20 °C

	rate constant/s^{-1}		
	solution	electrochemistry	
$[2Fe^{MIM}]$/μM	*Cr*HydA1	*Cr*HydA1	*Cp*I
0.0025	0.0097		
0.005	0.013	0.0066	
0.010	0.014	-	
0.028			0.0012
0.050	-	0.0104	
0.056			0.0014
0.100	-	0.0099	
0.110			0.0015
0.250	-	0.0060	
0.500	-	0.0072	
2.220			0.002

The rates are essentially independent of the already very low concentration of $[2Fe]^{MIM}$. The average rate constant for *Cr*HydA1 from all CA measurements is 0.008 s^{-1}, corresponding to a half-life of approximately 86 s, and the values are in reasonable agreement with those measured from the activation phase in solution assays. Analogous experiments with *Cp*I gave slower rates under similar conditions, with a typical rate constant of 0.002 s^{-1}. Importantly, there was no effect of light on the rates, thus showing that the species undergoing rate-determining conversion is not the same as the CO-inhibited state H_{ox}−CO, which is reactivated more rapidly under illumination.[10] In experiments carried out by Esselborn et al.[8] in which the reaction of $[2Fe]^{MIM}$ with apo-*Cr*HydA1 was monitored instead by the rate of CO release, the rate constant (pH 6.8, room temperature) was approximately 0.02 s^{-1}, somewhat higher than obtained using H_2 oxidation activity to monitor progress. From the temperature dependence of rate constants measured over the range 6−20 °C, activation parameters were as follows: *Cr*HydA1, $\Delta H^{\ddagger}$ = 46.2 ± 5.0 kJ mol^{-1}, $\Delta S^{\ddagger}$ = −134 ± 20 J K^{-1} mol^{-1}; *Cp*I, $\Delta H^{\ddagger}$ = 52.1. ± 3.0 kJ mol^{-1}, $\Delta S^{\ddagger}$ = −120 ± 20 J K^{-1} mol^{-1}.

The entire activation process starting from apo-[4Fe-4S] and $[2Fe]^{MIM}$ must involve binding, release of CO, formation of a μ-SCys bond between [2Fe] and cysteine thiolate, and any necessary additional rearrangements (but not necessarily in that order).

Some of these steps may also depend upon the oxidation state of apo-[4Fe-4S] and $[2Fe]^{MIM}$ or both, thus allowing diagnostic interruptions: hence experiments were carried out to investigate the potential dependence of the rate of activation. A PGE electrode modified with a film of apo-[4Fe-4S] (*Cr*HydA1 or *Cp*I) was held at different fixed potentials for approximately 500 s before an aliquot of $[2Fe]^{MIM}$ was injected to give a final concentration of 0.6 μM. For both enzymes, an increase in activity was observed immediately, provided the electrode potential was more positive than approximately −0.5 V vs SHE. Measurements at potentials close to the reversible $2H^+/H_2$ value suffered from low current amplitude; however, the general conclusion was that the rate of activation, viewed through H_2 oxidation, shows little potential dependence between −0.45 and 0 V. In contrast, barely any activation (detected as H^+ reduction) was observed when the electrode potential was held more negative than −0.5 V. These experiments suggested that active H-cluster formation is sensitive to the oxidation state of an intermediate species.

More detailed measurements were made over a longer time course to establish, more clearly, the threshold potential controlling activation. Instead of H_2, Ar was used, and the temperature was held at 5 °C to improve film stability. Representative results are shown in Figure 3. After forming a film of apo-[4Fe-4S], the electrode was held at the desired starting potential. To rule out the possibility that binding of apo-[4Fe-4S] to the electrode is potential dependent, the electrode was removed and rinsed thoroughly after approximately 6 min, fresh buffer introduced, and the electrode potential restored. An aliquot of $[2Fe]^{MIM}$ was then injected to a final concentration of 0.6 μM. At −0.54 V, only a very slow increase in H^+ reduction current was observed, showing that no activation was occurring; however, a short potential step to −0.04 V was sufficient to initiate activation (Figure 3A,B) which continued when the potential was stepped back to −0.54 V and thereafter regardless of potential (−0.04 or −0.54 V). Because H_2 was absent, each step to −0.04 V gives a zero current reading. In contrast, if the electrode potential was held at −0.44 V, activation was evident soon after upon injection of $[2Fe]^{MIM}$, more so for *Cp*I. Experiments (Supporting Information, Figure S1) in which a very negative potential was applied (<−0.69 V) were complicated by competing inactivation of the active hydrogenase under highly reducing conditions (as reported previously[18]) and could not be interpreted reliably. Consequently, we could not rule out a change in rate occurring at very negative potentials.

The observation of a threshold potential, in the region of approximately −0.4 to −0.5 V vs SHE, suggested that the redox level of the [4Fe-4S] cluster, either before *or* immediately following fusion by μ-SCys bond formation, might be a controlling factor. The $[4Fe\text{-}4S]^{2+/+}$ cluster in apo-*Cr*HydA1 is easily reducible by dithionite,[19] but to obtain more insight, the reduction potential was estimated by a potentiometric titration monitored using UV−visible spectrophotometry. A value of approximately −0.3 V vs SHE was obtained at pH 6.0 (Figure S2). Cyclic voltammetry of an aqueous solution of $[2Fe]^{MIM}$ revealed a quasi-reversible oxidation with a potential of −0.09 V vs SHE at pH 6.1, 15 °C (Figure S3). No other redox couples were observed between −560 mV and +240 mV. As a Fe(I) complex, $[2Fe]^{MIM}$ possesses 18 valence electrons on each Fe if a metal−metal bond is included in the electron count. Such compounds tend to be stable but lose CO upon oxidation.[20]

Next, it was important to establish if a stable precursor complex is formed between apo-[4Fe-4S] and $[2Fe]^{MIM}$ which cannot react further while it is held in a reduced state. We

DOI: 10.1021/jacs.6b09366
J. Am. Chem. Soc. 2016, 138, 15227−15233

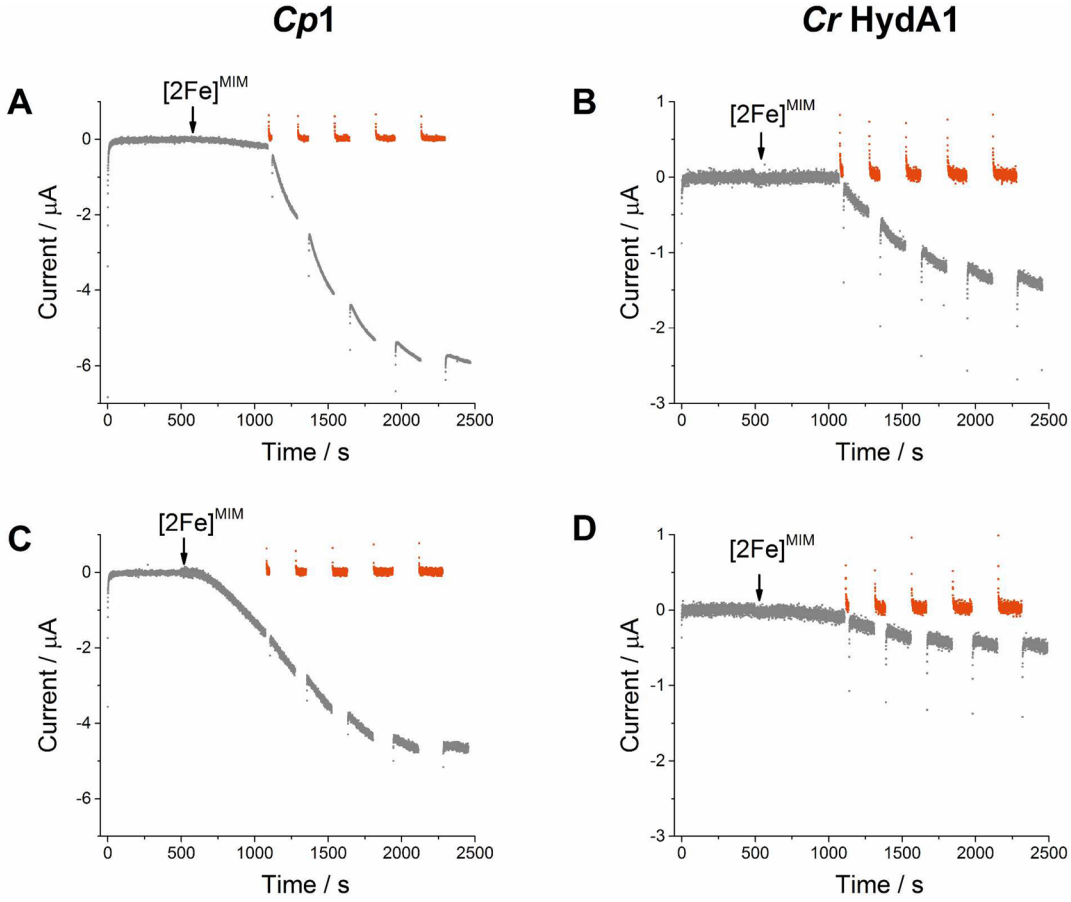

Figure 3. Chronoamperometry experiments showing how the activation of *Cp*I (left) and *Cr*HydA1 (right) by $[2Fe]^{MIM}$ is initiated by the electrode potential (5 °C, pH 6.0). (A) and (B) Voltage held at −0.54 V vs SHE (gray) initially for ∼1000 s, during which $[2Fe]^{MIM}$ was injected to a final concentration of 600 nM at ∼500 s. Potential stepped to −0.04 V (orange) for five separate intervals and returned to the starting potential, −0.54 V, between each interval to monitor the H^+ reduction activity. 100% Ar throughout; electrode rotated at 1000 rpm. (C) and (D) As for (A) and (B) with starting potential held at −0.44 V (in gray) and stepped periodically to −0.04 V (orange).

therefore exploited the ability of PFE to retain enzyme on the electrode while replacing solution species by buffer exchanges. Typically, a film of apo-[4Fe-4S] formed in the normal way was held at −0.54 V, and $[2Fe]^{MIM}$ was introduced to the cell. Any unbound $[2Fe]^{MIM}$ was then removed completely by a 10-fold buffer exchange, ensuring the electrode remained in contact with the cell solution to retain potential control. Upon stepping the electrode potential to −0.04 V then back to −0.54 V, the activity increased, as observed in experiments without a buffer exchange (Figure S4). This result, obtained using either *Cr*HydA1 or *Cp*I, confirmed that a very tightly bound intermediate must be formed between $[2Fe]^{MIM}$ and apo-[4Fe-4S] before activation is triggered by stepping the potential above the threshold value. The result is fully consistent with the fact that only extremely low $[2Fe]^{MIM}$ concentrations were required in all experiments.

We could thus conclude that $[2Fe]^{MIM}$ has a very high affinity for the apo-[4Fe-4S] enzyme in the earliest observable steps of the activation process, producing an intermediate that can be trapped, artificially, under reducing conditions. The fact that relaxing this condition initiates completion of activation shows that a second intermediate is also involved. A model consistent with all the data is shown in Scheme 1.

In the first stage, $[2Fe]^{MIM}$ enters apo-[4Fe-4S] to form a very stable complex (P), further processing of which is blocked if a potential <−0.54 V is applied. Under these conditions, therefore, P is reduced to P^{red}. The origin of the threshold potential is elusive as it refers to an unstable intermediate that is difficult to study independently. As a hypothesis, we propose that the threshold potential corresponds to the $[4Fe\text{-}4S]^{2+/+}$ couple. We estimated apo-[4Fe-4S] *Cr*HydA1 to have a potential in the region of −0.3 V, but this could shift to more negative values once $[2Fe]^{MIM}$ has entered the protein and taken up an adjacent position. The rate-determining step is conversion of the second intermediate Q to active enzyme. We now consider the likely options, in terms of (1) the nature of the step P → Q, (2) the point at which CO is released, and (3) relevance for the *in vivo* assembly process. Experiments have shown that the CO-inhibited H-cluster is destabilized when it is too electron rich (i.e., at the "super-reduced" redox level), and DFT calculations have suggested that the bond between the μSCys and the [2Fe] domain is broken.[12] Likewise, a structural analog of the H-cluster exhibits analogous cleavage of a Fe−μSR−Fe bond upon reduction.[21] It is therefore likely that the [2Fe−μSCys−4Fe] bond cannot form if the [4Fe-4S] cluster is reduced (and therefore electron-donating rather than electron-withdrawing) because the additional CO ligand on $[2Fe]^{MIM}$ renders the immediate product too electron-rich. This behavior is explained in terms of valence-electron counting because each Fe atom in $[Fe_2[\mu\text{-}(SCH_2)_2NH](CN)_2(CO)_4]^{2-}$ formally has 17 valence electrons if we ignore the metal−metal bond that may or may not be present. Formation of an

DOI: 10.1021/jacs.6b09366
J. Am. Chem. Soc. 2016, 138, 15227−15233

Scheme 1. Hypothesis for the Order of Events in the Formation of Active H-Cluster from apo-[4Fe−4S] and the Water-Soluble Synthetic Mimic [2Fe]^{MIM}

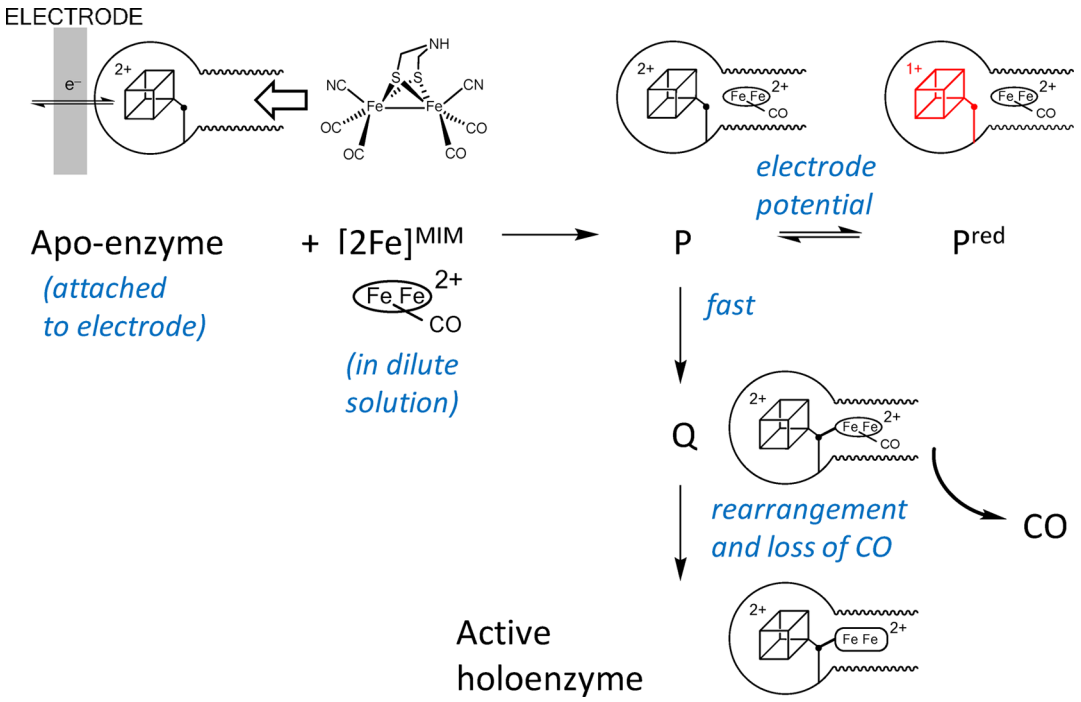

additional μSCys bond to one Fe (which adds 2 electrons to its valence shell) can be tolerated if the [4Fe-4S] cluster is oxidized (2+) because one electron can be shunted back to the cluster, yielding 18 and 17 valence electrons for proximal and distal Fe atoms, respectively. When the [4Fe-4S] cluster is reduced (1+) such a shunt is not possible, and the only option is to transfer an electron from the proximal Fe to the distal Fe, making the latter formally Fe(0), which is less likely given the presence of cyanide and thiolate ligands that coordinate because they are good donors to metal cations. In such a scenario, the transition P → Q represents the step in which 2Fe^{MIM} fuses covalently with the [4Fe-4S] cluster. Release of CO could occur at any stage after fusion, but three observations need to be considered. First, the lack of light sensitivity on the activation rate shows that CO release does not occur from a species that is a recognized CO-inhibited form[10] but occurs as part of a more complex process of adjustment. Second, the very negative activation entropies suggest a well-organized transition state, arguing against the rate-determining step being simply the release of CO or expulsion of solvent that may have already occurred upon initial formation of P.[2] Third, all our studies so far indicate that CO release is somewhat faster than activation, so CO is released during or before the rate-determining step. Bringing all evidence together, the rate-determining step for achieving active enzyme, regardless of whether assembly is occurring in *Cp*I or *Cr*HydA1, most likely involves final rearrangement of the 2Fe coordination shell.

The fact that intermediate P already has the 2Fe complex bound very tightly, despite the strong likelihood that it is not yet covalently bound, is striking. The binding might be electrostatically favored in the "open" structure (exemplified in the crystal structure of apoHydA1,[4] which contains an open cationic channel 25 Å deep, between 8 and 15 Å in width, and lined by an evolutionary conserved arginine and two conserved lysines that can interact strongly with the dianionic [2Fe]^{MIM} guest. Similarly, the [2Fe]^{MIM} could be accommodated by the binding site, which is highly preorganized, as supported by close similarities between *Cp*I and the "closed" structure seen in crystals of apo-[4Fe-4S] *Cp*I.[5]

In the physiological process, the molecular structure of the entity that is formed on HydF and transferred to HydA is currently unknown but is likely to resemble 2Fe^{MIM} in both structure and charge. In terms of ligand content, the only difference in composition between 2Fe^{MIM} and the [2Fe] complex in HydA is the presence of an extra CO. Evidence from FTIR indicates that all four CO ligands are retained when HydF is either loaded naturally or when [2Fe]^{MIM} binds to HydF.[6,22] In addition, EPR measurements of both semi-synthetic and naturally loaded HydF show that the [2Fe] complex is diamagnetic, consistent with a Fe(I)−Fe(I) redox state.[6,23] Whatever species is actually transferred, it must be sufficiently stable to survive brief exposure to solvent water without decomposition. If, indeed, the transferring species is identical to 2Fe^{MIM}, then each of the intramolecular steps from P onward, which appear similar regardless of the enzyme, should apply equally well for *in vivo* assembly. In summary, our investigations, which reveal a tightly bound early intermediate that can be artificially trapped by imposing highly reducing conditions, lead to an "order-of-events" mechanistic model to aid detailed time-resolved spectroscopic examinations at the atomic level.

EXPERIMENTAL SECTION

ApoHydA1 and apoCpI were overexpressed in *E. coli* BL21 (DE3) ΔiscR[24] as described previously[25] and purified by strep-tactin affinity chromatography under strictly anoxic conditions.[5] The water-soluble $[Fe_2[\mu\text{-}(SCH2)_2NH](CN)_2(CO)_4]^{2-}$ complex was synthesized and purified as reported before.[5,6]

To estimate the midpoint potential of apoHydA1, a solution of 50 μM protein in 0.5 M MES pH 6.0 with 0.1 mM methylviologen was prepared, and the open-circuit potential (OCP) was monitored

DOI: 10.1021/jacs.6b09366
J. Am. Chem. Soc. 2016, 138, 15227−15233

continuously with a Reference 600 potentiostat (GAMRY) using a gold electrode with a Pt-counter electrode and Ag/AgCl (3 M) reference electrode under completely anaerobic conditions. The potential was adjusted by titration with sodium dithionite while stirring. Upon stabilization of the OCP, a sample was taken and the absorbance measured between 250 and 600 nm (Smart Spec 3000, Biorad). Spectra were digitally smoothed and corrected for volume changes due to additions of dithionite solution. The variation of absorption with potential was plotted for selected wavelengths and fitted to the Nernst equation.

All chemicals were of analytical grade, and solutions were prepared using purified water (Millipore, 18 MΩ cm). Phosphate buffer was prepared by titration of the monobasic and dibasic forms (Sigma-Aldrich or Acros Organics) until the desired pH was attained. Protein film electrochemistry experiments were carried out in an anaerobic glovebox (MBraun 150B-G) in an N_2 atmosphere (O_2 < 2 ppm). Electrochemical measurements were made using an Autolab potentiostat (PGSTAT128N) with Nova software (EcoChemie). The gastight electrochemical cell was fitted with a water jacket, to ensure a constant temperature. The working electrode was a pyrolytic graphite rotating disc electrode controlled by a rotator (EcoChemie) with a constant rotation speed of 1000 rpm. The reference electrode (saturated calomel electrode, SCE) was held in a nonisothermal side arm containing either 0.1 M NaCl (for rate experiments) or the buffer used in the main cell compartment (for the potential-dependent experiments); it was connected to the main cell compartment by a luggin capillary. Platinum wire was used as the counter electrode. The reference potential was converted to the standard hydrogen electrode (SHE) scale using the correction $E_{SHE} = E_{SCE} + 0.241$ at 25 °C.[26] Precise gas mixtures (BOC gases) in each experiment were provided by use of mass flow controllers (Sierra Instruments).

To prepare the working electrode for use in each experiment, the PGE surface was abraded with p400 Tufbak Durite sandpaper, wiped with tissue, and briefly sonicated to remove excess carbon before rinsing with deionized water. Apo-enzyme was then adsorbed onto the electrode by spotting 2 μL of a 25 μM solution of apoenzyme directly onto the graphite for approximately 1−2 min, before rinsing with purified water to remove any excess enzyme.

In cyclic voltammetry experiments the potential was swept linearly between upper and lower limits with a typical scan rate of 30 mV s^{-1}. In chronoamperometry experiments the potential was held constant at the starting value. After approximately 500 s, the program was paused, and the electrode (still connected to the rotator) was removed from the cell solution, rinsed thoroughly, and stored in buffer. The solution in the cell was then exchanged for fresh buffer, the electrode was reinserted into the cell, and the program resumed. This wash step ruled out the possibility that binding of apoenzyme to the electrode was potential dependent, since any apoenzyme which may have dissociated from the electrode while being held at the chosen potential during the first stage of the experiment would be removed. Activation of apoenzyme after this step confirmed that the enzyme had not dissociated from the electrode, and therefore the potential dependence observed was not related to the enzyme failing to bind to the electrode at very negative potentials. On resuming the program, $[2Fe]^{MIM}$ was injected into the cell to a final concentration of 0.6 μM and the voltage again held at the starting potential (before the wash step). After a further 500 s, the voltage was stepped to −0.04 V vs SHE for five separate intervals (with increasing lengths of time), and after each interval it was returned to the original starting potential to monitor the reduction of H^+; 100% argon was used throughout.

Some potential-dependent experiments included a buffer exchange step after the injection of mimic (Figure S4). The cell solution was allowed to drip out of the electrochemical cell by replacing the gas outlet with a syringe containing 40 mL of buffer which had previously been incubated at 5 °C. The inlet gas remained on, and the resulting increase in pressure caused the solution to exit the cell through a third needle. At the same time, the new buffer was injected into the cell until the original 4 mL cell solution had been replaced 10 times. During the buffer exchange, the electrode remained in contact with the cell solution, therefore retaining potential control. The buffer exchange at this point in the experiment removed completely any unbound $[2Fe]^{MIM}$.

Additional control experiments confirmed that the 10-fold exchange was adequate for complete removal of the unbound $[2Fe]^{MIM}$; the cell solution following buffer exchange was tested for the presence of $[2Fe]^{MIM}$ by insertion of an electrode with freshly adsorbed apoenzyme. Activation did not occur during successive cyclic voltammograms, confirming the absence of $[2Fe]^{MIM}$ in the solution. Injection of fresh $[2Fe]^{MIM}$ into the solution activated the newly adsorbed apoenzyme, ruling out the possibility that the previously observed inactivity was due to unsuccessful adsorption onto the electrode.

Activation parameters were determined by analysis of the rates of activation and recorded for the H_2 oxidation direction, at different temperatures using the Eyring equation. Accounting for the Nernstian dependence of $E_{2H+/H2}$ with temperature, all experiments were carried out at 150 mV above $E_{2H+/H2}$ ($E_{2H+/H2}$ = −342 mV at pH 6.0, 15 °C in 100% H_2). This potential provided a driving force that maintained H_2 oxidation activity while remaining below the potential at which oxidative inactivation occurs.

For the kinetic experiments carried out in solution, rates of oxidation of H_2 were measured by conventional protocols, monitoring the reduction of benzyl viologen (Sigma-Aldrich) at 600 nm. Experiments were carried out in an anaerobic glovebox (O_2 < 2 ppm) (Belle Technologies) using an Ocean Optics S2000 fiber optic spectrophotometer controlled with OOIBase32 software (Ocean Optics, Inc.) at room temperature (20−22 °C). Benzyl viologen (Sigma-Aldrich) was dissolved to a stock concentration of 10 mM in 0.1 M potassium phosphate buffer (pH 6.8) and diluted for subsequent assays using the same buffer. The working solution of benzyl viologen was continuously purged with H_2 in a sealed glass vial for at least 5 min before each experiment. Then 1 mL of H_2-saturated benzyl viologen was injected into a sealed cuvette (containing a magnetic stirrer flea) into which was placed a H_2 inlet needle and an outlet needle to the headspace; the starting absorbance was monitored until stable. Apo-enzyme was then drawn into a gastight Hamilton syringe and injected into the sealed cuvette and the absorbance was monitored until stable. After this time $[2Fe]^{MIM}$ was injected to the desired final concentration using a separate Hamilton syringe to avoid mixing apoenzyme and $[2Fe]^{MIM}$ beforehand. Immediately after injection of $[2Fe]^{MIM}$, thorough mixing was achieved by bubbling H_2 directly into the solution by insertion of the inlet needle. Apo-enzyme and $[2Fe]^{MIM}$ were diluted to stock concentrations such that the volume added to the cuvette each time was constant at 5 μL for both. The rate of reduction of benzyl viologen by H_2 is proportional to the amount of active hydrogenase generated. Absorbance values were converted to concentration using the Beer−Lambert law with a molar extinction coefficient of 7400 M^{-1} cm^{-1} at 600 nm.[27] The primary plots were smoothed using the adjacent-averaging function in Origin, and the first derivative of this smoothed data was obtained. The first derivative data were smoothed using the adjacent-averaging function and then fitted to an exponential ($y = y_0 + A*\exp(R_0*x)$ in Origin.

■ ASSOCIATED CONTENT

Supporting Information

The Supporting Information is available free of charge on the ACS Publications website at DOI: 10.1021/jacs.6b09366.

Chronoamperometry showing the potential dependence of activation of *Cp*I and *Cr*HydA1 by $[2Fe]^{MIM}$ at very negative potentials. Estimation of reduction potential of apo-[4Fe−4S] *Cr*HydA1 and $[2Fe]^{MIM}$. Chronoamperometry to study effect of buffer exchange (PDF)

■ AUTHOR INFORMATION

Corresponding Author

*fraser.armstrong@chem.ox.ac.uk

DOI: 10.1021/jacs.6b09366
J. Am. Chem. Soc. 2016, 138, 15227−15233

Notes

The authors declare no competing financial interest.

■ ACKNOWLEDGMENTS

This research was supported by the ERASynBio consortium "Sun2Chem". F.A.A. thanks the UK Biotechnology and Biological Sciences Research Council for funding (grant BB/M005720/1). T.H. gratefully acknowledges support from the Deutsche Forschungsgemeinschaft (Cluster of Excellence RESOLV, EXC1069 and DIP project cooperation "Nano-engineered optoelectronics with biomaterials and bioinspired assemblies") and the Volkswagen Foundation (LigH2t).

■ REFERENCES

(1) Lubitz, W.; Ogata, H.; Rüdiger, O.; Reijerse, E. *Chem. Rev.* **2014**, *114*, 4081−4148.
(2) Shepard, E. M.; Mus, F.; Betz, J. N.; Byer, A. S.; Duffus, B. R.; Peters, J. W.; Broderick, J. B. *Biochemistry* **2014**, *53*, 4090−4104.
(3) Shepard, E. M.; Byer, A. S.; Betz, J. N.; Peters, J. W.; Broderick, J. B. *Biochemistry* **2016**, *55*, 3514−3527.
(4) Mulder, D. W.; Boyd, E. S.; Sarma, R.; Lange, R. K.; Endrizzi, J. A.; Broderick, J. B.; Peters, J. W. *Nature* **2010**, *465*, 248−U143.
(5) Esselborn, J.; Muraki, N.; Klein, K.; Engelbrecht, V.; Metzler-Nolte, N.; Apfel, U. P.; Hofmann, E.; Kurisu, G.; Happe, T. *Chem. Sci.* **2016**, *7*, 959−968.
(6) Berggren, G.; Adamska, A.; Lambertz, C.; Simmons, T. R.; Esselborn, J.; Atta, M.; Gambarelli, S.; Mouesca, J. M.; Reijerse, E.; Lubitz, W.; Happe, T.; Artero, V.; Fontecave, M. *Nature* **2013**, *499*, 66−9.
(7) Li, H.; Rauchfuss, T. B. *J. Am. Chem. Soc.* **2002**, *124*, 726−727.
(8) Esselborn, J.; Lambertz, C.; Adamska-Venkatesh, A.; Simmons, T.; Berggren, G.; Noth, J.; Siebel, J.; Hemschemeier, A.; Artero, V.; Reijerse, E.; Fontecave, M.; Lubitz, W.; Happe, T. *Nat. Chem. Biol.* **2013**, *9*, 607−609.
(9) Hexter, S. V.; Grey, F.; Happe, T.; Climent, V.; Armstrong, F. A. *Proc. Natl. Acad. Sci. U. S. A.* **2012**, *109*, 11516−11521.
(10) Goldet, G.; Brandmayr, C.; Stripp, S. T.; Happe, T.; Cavazza, C.; Fontecilla-Camps, J. C.; Armstrong, F. A. *J. Am. Chem. Soc.* **2009**, *131*, 14979−14989.
(11) Stripp, S. T.; Goldet, G.; Brandmayr, C.; Sanganas, O.; Vincent, K. A.; Haumann, M.; Armstrong, F. A.; Happe, T. *Proc. Natl. Acad. Sci. U. S. A.* **2009**, *106*, 17331−17336.
(12) Baffert, C.; Bertini, L.; Lautier, T.; Greco, C.; Sybirna, K.; Ezanno, P.; Etienne, E.; Soucaille, P.; Bertrand, P.; Bottin, H.; Meynial-Salles, I.; De Gioia, L.; Léger, C. *J. Am. Chem. Soc.* **2011**, *133*, 2096−2099.
(13) Parkin, A.; Cavazza, C.; Fontecilla-Camps, J. C.; Armstrong, F. A. *J. Am. Chem. Soc.* **2006**, *128*, 16808−16815.
(14) Hambourger, M.; Gervaldo, M.; Svedruzic, D.; King, P. W.; Gust, D.; Ghirardi, M.; Moore, A. L.; Moore, T. A. *J. Am. Chem. Soc.* **2008**, *130*, 2015−2022.
(15) Madden, C.; Vaughn, M. D.; Díez-Pérez, I.; Brown, K. A.; King, P. W.; Gust, D.; Moore, A. L.; Moore, T. A. *J. Am. Chem. Soc.* **2012**, *134*, 1577−1582.
(16) Armstrong, F. A.; Evans, R. M.; Hexter, S. V.; Murphy, B. J.; Roessler, M. M.; Wulff, P. *Acc. Chem. Res.* **2016**, *49*, 884−892.
(17) Fourmond, V.; Greco, C.; Sybirna, K.; Baffert, C.; Wang, P. H.; Ezanno, P.; Montefiori, M.; Bruschi, M.; Meynial-Salles, I.; Soucaille, P.; Blumberger, J.; Bottin, H.; De Gioia, L.; Léger, C. *Nat. Chem.* **2014**, *6*, 336−342.
(18) Hajj, V.; Baffert, C.; Sybirna, K.; Meynial-Salles, I.; Soucaille, P.; Bottin, H.; Fourmond, V.; Léger, C. *Energy Environ. Sci.* **2014**, *7*, 715−719.
(19) Mulder, D. W.; Ortillo, D. O.; Gardenghi, D. J.; Naumov, A. V.; Ruebush, S. S.; Szilagyi, R. K.; Huynh, B.; Broderick, J. B.; Peters, J. W. *Biochemistry* **2009**, *48*, 6240−6248.
(20) Boyke, C. A.; van der Vlugt, J. I.; Rauchfuss, T. B.; Wilson, S. R.; Zampella, G.; De Gioia, L. *J. Am. Chem. Soc.* **2005**, *127*, 11010−11018.
(21) Tard, C.; Liu, X. M.; Ibrahim, S. K.; Bruschi, M.; De Gioia, L.; Davies, S. C.; Yang, X.; Wang, L. S.; Sawers, G.; Pickett, C. J. *Nature* **2005**, *433*, 610−613.
(22) Czech, I.; Silakov, A.; Lubitz, W.; Happe, T. *FEBS Lett.* **2010**, *584*, 638−642.
(23) Shepard, E. M.; McGlynn, S. E.; Bueling, A. L.; Grady-Smith, C. S.; George, S. J.; Winslow, M. A.; Cramer, S. P.; Peters, J. W.; Broderick, J. B. *Proc. Natl. Acad. Sci. U. S. A.* **2010**, *107*, 10448−10453.
(24) Akhtar, M. K.; Jones, P. R. *Appl. Microbiol. Biotechnol.* **2008**, *78*, 853−862.
(25) Kuchenreuther, J. M.; Grady-Smith, C. S.; Bingham, A. S.; George, S. J.; Cramer, S. P.; Swartz, J. R. *PLoS One* **2010**, *5*, 7.
(26) Bard, A. J.; LR, F. *Electrochemical Methods: Fundamentals and Applications*; Wiley, 2001.
(27) Ballantine, S. P.; Boxer, D. H. *J. Bacteriol.* **1985**, *163*, 454−459.

DOI: 10.1021/jacs.6b09366
J. Am. Chem. Soc. 2016, 138, 15227−15233